

Supplementary Information for

## **Protease inhibition mechanism of camelid-like synthetic human antibodies**

Dong Hyun Nam<sup>1</sup>, Ki Baek Lee<sup>1</sup>, Evan Kruchowy, Henry Pham, Xin Ge\*

Department of Chemical and Environmental Engineering  
University of California, Riverside  
900 University Ave  
Riverside, CA 92521 USA

\*Corresponding Author, Email: [xge@engr.ucr.edu](mailto:xge@engr.ucr.edu)

1. These authors contributed equally to this work.

### **Table of Content**

**Figure S1.** SDS-PAGE of purified Fabs

**Figure S2.** Binding kinetics of Fabs on cdMMP-14

**Figure S3.** Active-site of cdMMP-14

**Figure S4.** nTIMP-2 binding surface on cdMMP-14

**Figure S5.** Competitive ELISA with GM6001

**Figure S6.** Production of cdMMP14 alanine point mutants

**Figure S7.** Additional exemplary results of competitive ELISA

**Figure S8.** Production of Fab 3A2 mutants

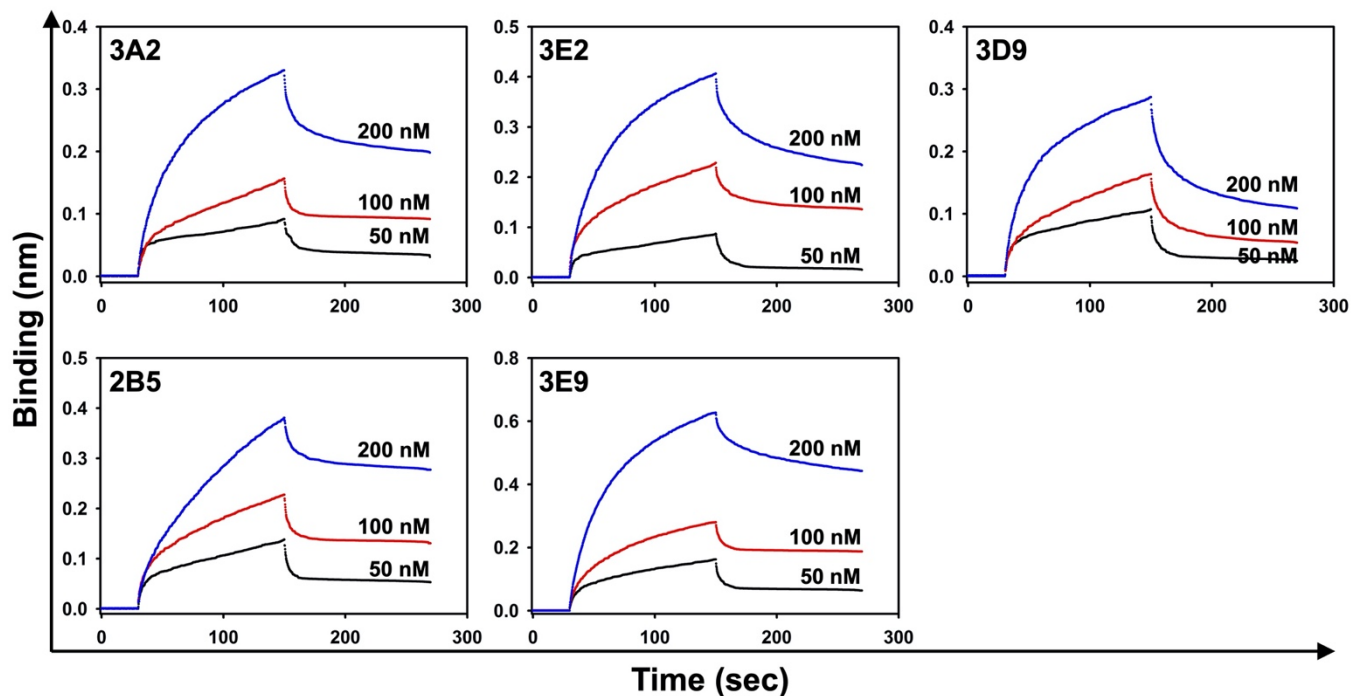
**Figure S9.** Biolayer interferometry results of Fab 3A2 mutants

Figure S1:



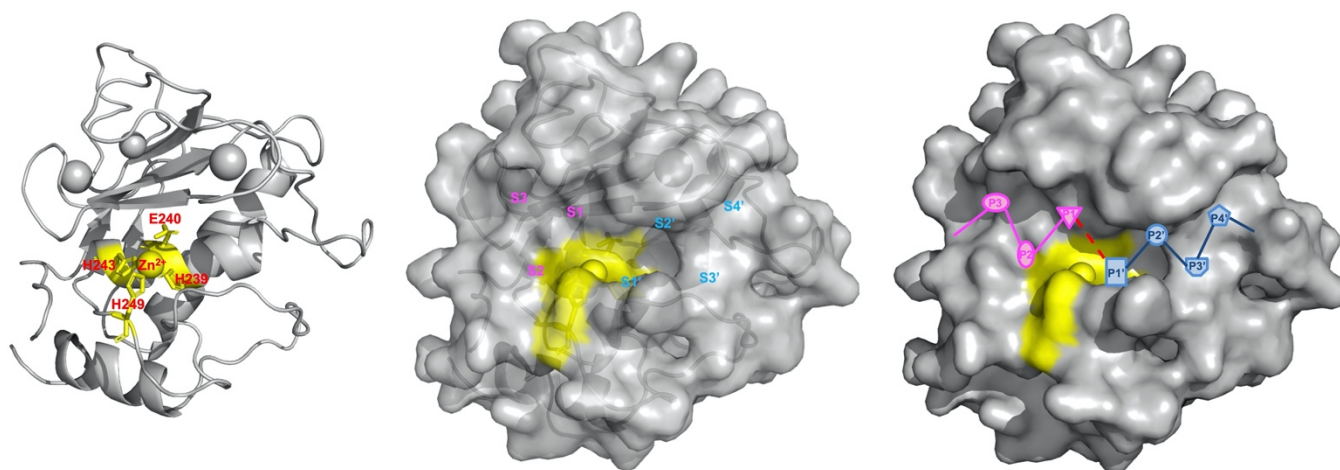
**Figure S1. SDS-PAGE of purified Fabs.** Fabs were expressed in periplasmic space of *E. coli* BL21 cells and purified by using Ni-NTA chromatography. Purified Fabs were analyzed by SDS-PAGE at non-reducing condition.

Figure S2:



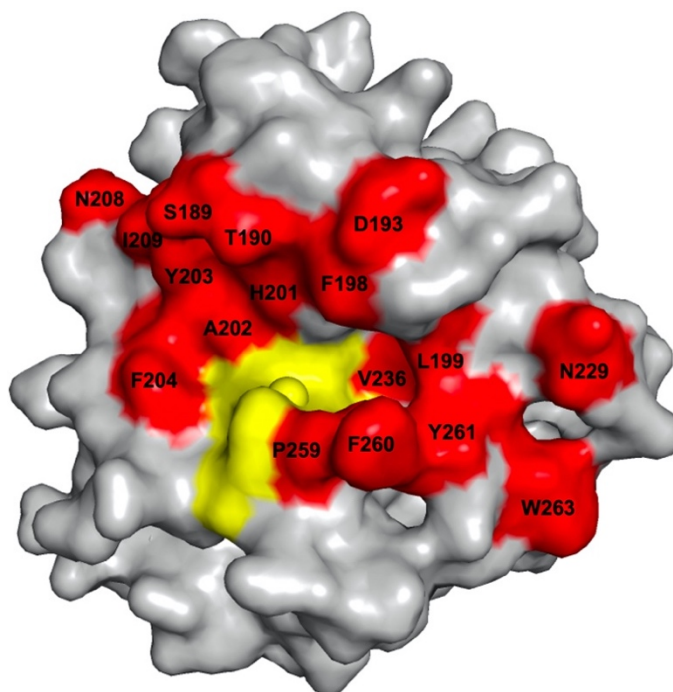
**Figure S2. Binding kinetics of Fabs on cdMMP-14.** Association constants ( $k_{on}$ ) and dissociation constants ( $k_{off}$ ) were determined by using biolayer interferometry (BLI) with biotinylated cdMMP-14 immobilized on streptavidin sensor, and values of binding affinity  $K_D$  were calculated.

**Figure S3:**



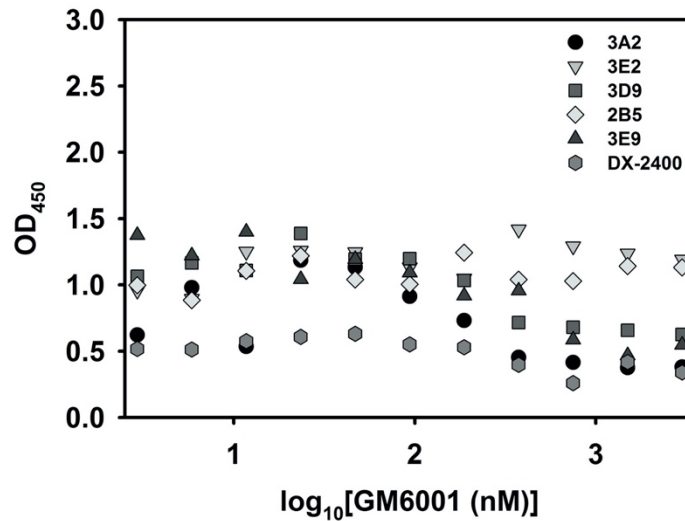
**Figure S3. Active cleft of MMP-14. (Left)** Catalytic zinc and its coordinating residues form the active site of MMP-14. **(Middle)** Located at either side of the catalytic zinc, the prime subsites (in pink) and the non-prime subsites (in blue) sculpt a cleft-like structure on the surface of cdMMP-14. **(Right)** A conceptual polypeptide substrate is accommodated within the cleft structure, promoting hydrolysis of the scissile bond between its P1 and P1' positions.

**Figure S4:**



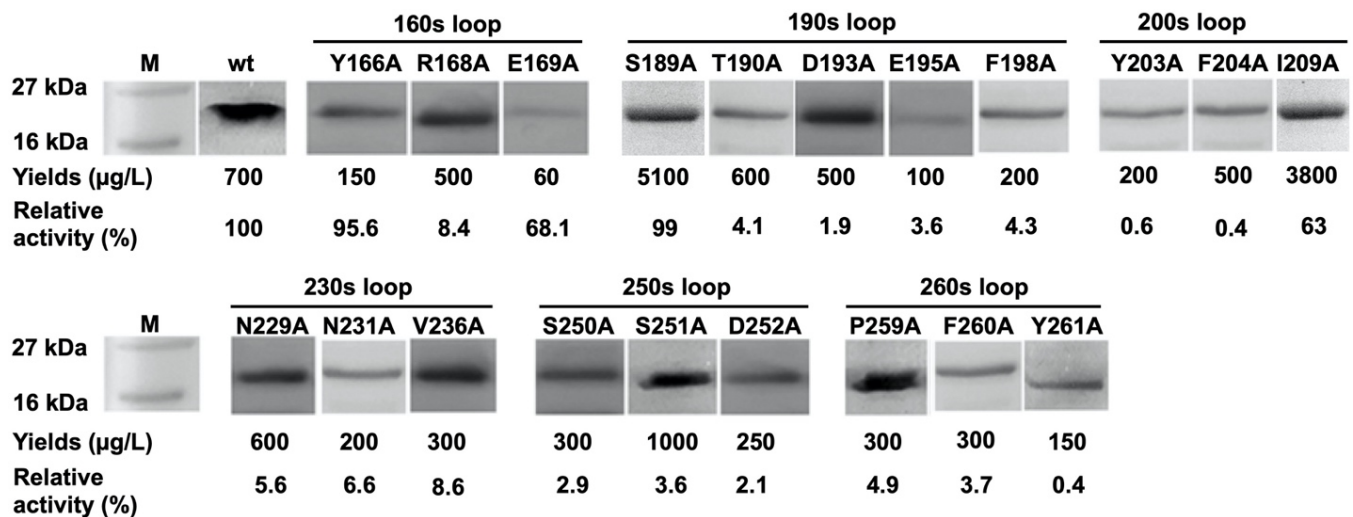
**Figure S4. nTIMP-2 binding surface on cdMMP-14.** The residues interacting with nTIMP-2 are in red. Catalytic zinc and its coordinating histidines (His239, His243 and His249) are in yellow. PDB=1BQQ.

Figure S5:



**Figure S5. Competitive ELISA with GM6001.** Immobilized cdMMP-14 was incubated with mixtures of 200 nM of Fabs (3A2, 3D9, and DX-2400) or 1  $\mu$ M of Fabs (3E2, 2B5, and 3E9) and 3 nM - 3  $\mu$ M GM6001. Signals were developed with anti-Fab-HRP.

Figure S6:



**Figure S6. Production of cdMMP14 alanine point mutants.** SDS-PAGE of produced cdMMP-14 mutants. Each cdMMP-14 mutants were cloned, periplasmically expressed and purified. Yields and enzymatic activities were measured to compare with wt cdMMP-14.

Figure S7:

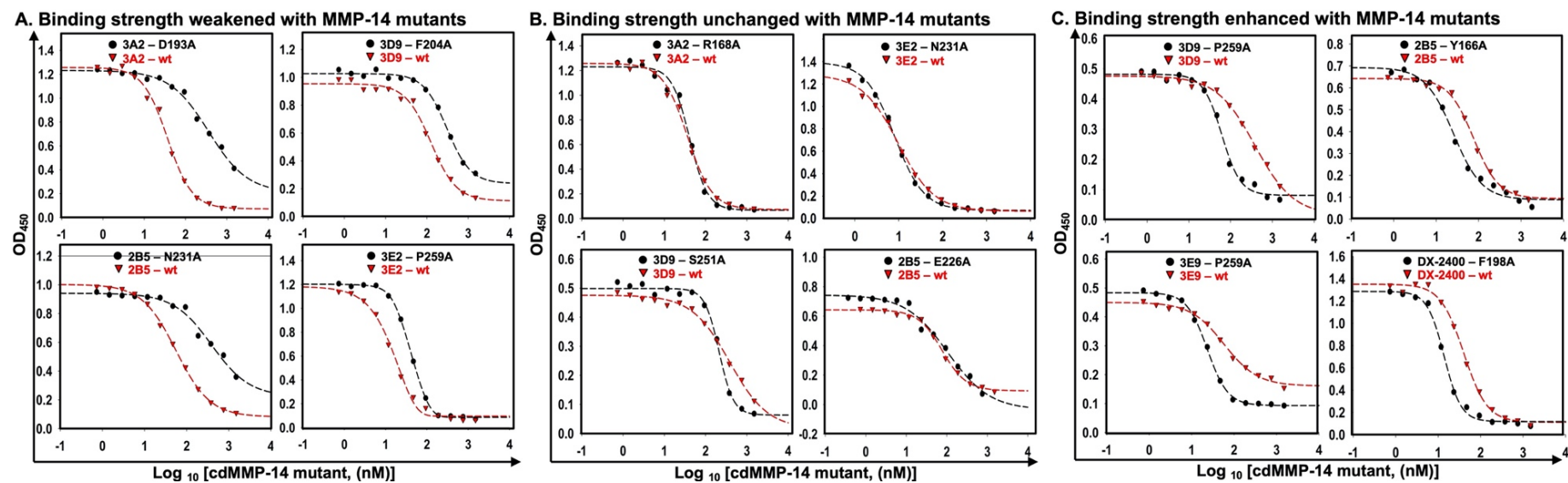


Figure S7. Additional exemplary results of competitive ELISA. Binding strength (A) weakened, (B) unchanged or (C) enhanced with MMP-14 mutants.

Figure S8:

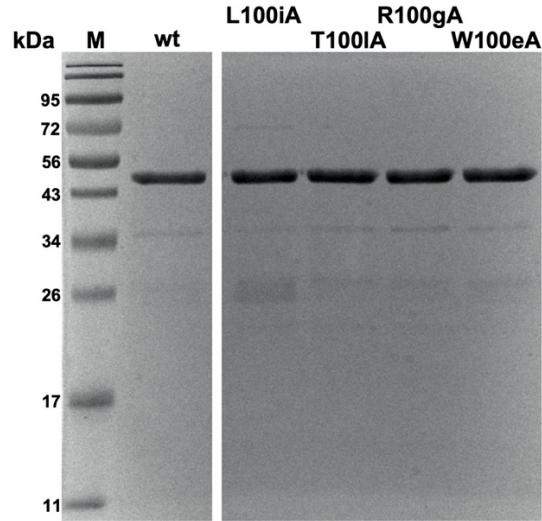


Figure S8. Production of Fab 3A2 mutants. Fabs were periplasmically expressed and purified Fabs were analyzed by SDS-PAGE at non-reducing condition.

Figure S9:

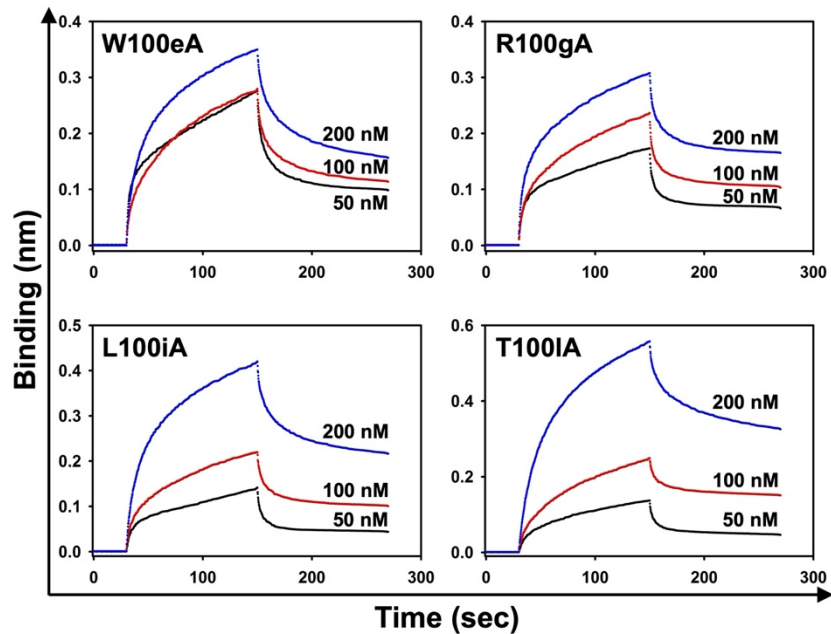


Figure S9. Biolayer interferometry results of Fab 3A2 mutants. Biotinylated cdMMP-14 was immobilized on streptavidin sensor and binding kinetics of Fabs, i.e.  $k_{on}$  and  $k_{off}$  were measured to determine affinity  $K_D$ .